Published by JScE as Proceedings of 4th International Conference on Earthquake Engineering and Post-Disaster Reconstruction Planning (ICEE-PDRP), 19-21 Jan. 2026, Bhaktapur, Nepal

DIGITAL HERITAGE DOCUMENTATION: INTEGRATING PHOTOGRAMMETRY, GAUSSIAN SPLATTING, AND 3D MESH MODELING PRACTICES FOR ENHANCED DETAIL AND EFFICIENCY

Asim Koirala[1*], **Rabina Shilpakar**[2]

[1] Zero Dia Design, Kathmandu, Nepal
[2] Department of Architecture, Khwopa Engineering College, Purbanchal University, Nepal

Abstract

Nepal's rich architectural heritage is under increasing threat from environmental changes and rapid modernization, highlighting the urgent need for advanced digital preservation methods. Digital architectural and cultural heritage documentation has been evolving, yet the current practices remain limited to their ability to capture detailed structural representation and material nuances combined with its ability to scale and easily deploy. This study explores a hybrid approach that integrates photogrammetry, Gaussian splatting and contemporary 3D mesh modelling workflows to enhance visual fidelity and precise digital replicas. Photogrammetry is recognized for its geometric accuracy but can be computationally demanding and struggle to capture reflective and transparent surfaces. While Gaussian splatting offers fast and high- fidelity visualizations but it's integration with existing modelling pipelines is ongoing. By combining these methods, this study suggests a flexible and potentially more scalable workflow that leverages strength of each technique. Preliminary applications to small monuments indicate improvement in visual fidelity and processing efficiency that captures nuanced material details. Since this workflow requires only photos, it presents a low-barrier option for broader application. For the case study of this workflow, a set number of Nepalese architectural heritage and monuments will be photographed, processed and compared with existing workflows in terms of its visual fidelity & computational demand.

Keywords: Digital Documentation; Photogrammetry; Gaussian splatting; 3D mesh modeling; Computational efficiency

1. Introduction

1.1. Significance of Cultural Heritage Documentation

Cultural heritage documentation serves as the foundation for preservation, restoration, and knowledge transmission across generations (Letellier, 2007). In Nepal, architectural heritage embodies centuries of artistic achievement through intricate wood carvings and religious monuments. However, these structures face accelerating deterioration from seismic activity, weathering, and modernization (Tiwari, 2009). The 2015 Gorkha earthquake destroyed over 750 historic structures, underscoring the critical need for comprehensive documentation that enables accurate reconstruction (Angelini et al., 2016).

Digital documentation has emerged as essential for creating permanent records, supporting condition assessment, structural analysis, restoration planning, and educational outreach (Champion, 2015; Remondino, 2011).

1.2. Limitations of Conventional Approaches

Traditional documentation methods present significant constraints. Manual measurements are time-consuming and unable to capture complex geometries effectively. Terrestrial laser scanning (TLS) and LiDAR, though precise, remain costly and require specialized equipment, limiting their use in extensive or remote heritage sites. These limitations highlight the need for more adaptable, image-based techniques that balance accuracy, scalability, and efficiency in heritage documentation.

*Corresponding author: Asim Koirala
Zero Dia Design, Kathmandu, Nepal
Email: asimkoirala123@gmail.com
https://doi.org/10.3126/jsce.v13i1.89578

1.3. Advances in Digital Capture and Representation

Photogrammetry has become one of the most accessible methods for 3D heritage documentation, generating detailed and metrically accurate models from overlapping photographs through Structure-from-Motion and Multi-View Stereo workflows (Westoby et al., 2012). Its versatility and low equipment requirements make it well suited for documenting heritage structures in diverse conditions.

Recent developments in rendering technology, particularly 3D Gaussian Splatting, offer an alternative that emphasizes visual fidelity and real-time performance. This approach enables high-quality spatial visualization with reduced computational demand, providing an efficient means to archive and present complex architectural forms (Gudon and Lepetit, 2024).

1.4. Scope and Objectives

This research evaluates three complementary techniques—photogrammetry, Gaussian splatting, and 3D mesh modeling—establishing their distinct roles for heritage conservation. Primary objectives include:

- Design a pipeline to integrate photogrammetry, 3D Gaussian splatting and manual 3D modeling in a single comprehensive heritage documentation workflow.
- Assess geometric accuracy of photogrammetric reconstruction against measured ground truth
- Evaluate Gaussian splatting as an archival tool for visual fidelity.
- Compare processing efficiency across workflows.
- Analyze conservation usability for BIM, VR/AR integration.

2. Methodology

2.1. Case Study Objects

Three heritage elements representing distinct typologies were selected (Figure 1):

a. **Newari window:** A lattice window (4.5m $\times$ 12m) with intricate geometric patterns and elements as thin 1.5cm.

b. **Chaitya:** A chaitya (2.6m $\times$ 2.6m $\times$ 3m) made up of stone with carvings.

c. **Chilancho stupa:** Chilancho Stupa in Kirtipur is a 15th-century Buddhist monument standing about 10.5m high on a stepped 48.2m $\times$ 48.2m quadrangular plinth with four corner chaityas. It features a white hemispherical dome, harmika, and tiered spire, reflecting the classic nepali chaitya style.

2.2. Data Acquisition

Image capture: Cannon Eos 1300d with 18-55 mm lens with tripod was used for the photography, 70-80% lateral overlap, and photographing in concentric circles to capture all the details. RAW file format was used for feasibility of post processing the images, white balance was set using 18% grey card. The settings for the camera were manual focus, ISO 100-200, f/stop 8-11 and shutter speed was kept as fast as possible. For the areas that were inaccessible like roofs and high areas, DJI Mini 4 Pro drone was used with similar camera settings. Georeferencing was used as ground control points.

Measured Ground Truth: Manual measurements using steel tape ($\pm$2mm), digital calipers ($\pm$0.01mm) established dimensional references at key points.

Environmental challenges: Real-world conditions included variable lighting, material reflectivity, shadow occlusion, and uniform surface textures, providing authentic testing scenarios for workflow reliability.

2.3. Workflow Approaches

2.3.1 Photogrammetry for Retrieving Fine Details in Mesh Form and Textures

RAW images were first edited in Lightroom and then processed in Reality Scan for image alignment, point cloud generation, meshing, and texturing. The generated 3D model was exported as an .obj file and further refined in Blender. To optimize the mesh (Figure 2 and 3), it was converted into a low-poly version using the free Instant Meshes software. High-resolution textures and fine details from the original high-poly model were then baked onto the simplified model in Blender using the Simple Bake add-on.

2.3.2 Gaussian Splatting for Archival Fidelity

For Gaussian splatting, the same photographs, along with point cloud and camera alignment data from RealityCapture, were imported into Jawset Postshot. This ensured consistency of camera poses across both pipelines. Processing was performed on an Nvidia RTX 3060 Laptop GPU, using the Splat MCMC radiance field profile for fast training. Images were down sampled to 1600 pixels, the maximum splat count was set at 1000, and training was stopped after 40k steps. The output .ply file sizr was very large, so it was converted to. spz format via StorySplat for file size reduction without compromising quality. For visualization (Figure 4 and 5), WebGL-based viewing was carried out using the SuperSplat website to examine as an option for a tool to view the high visual fidelity output that is accessible to public. Unreal Engine was used for the application for VR/AR use.

(a) (b) (c)

Figure 1. Photographs of (a) Newari Window (b) Chaitya (c) Chilancho Stupa

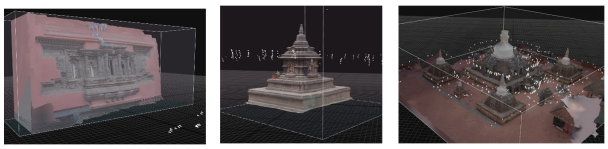

(a) (b) (c)

Figure 2. Photogrammetry mesh with textures (a) Newari Window (b) Chaitya (c) Chilancho Stupa

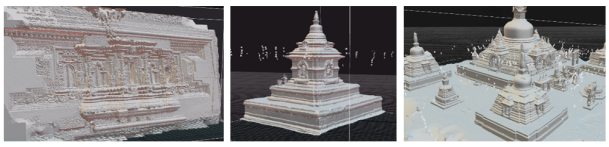

(a) (b) (c)

Figure 3. Photogrammetry mesh without textures (a) Newari Window (b) Chaitya (c) Chilancho Stupa

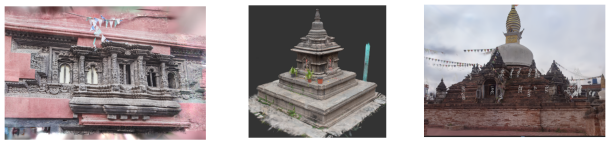

(a) (b) (c)

Figure 4. 3D gaussian splat of (a) Newari Window (b) Chaitya (c) Chilancho Stupa

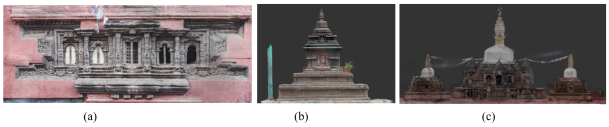

(a) (b) (c)

Figure 5. Elevations derived from gaussian splatting of (a) Newari Window (b) Chaitya (c) Chilancho Stupa

2.3.3 3D Modeling & Drafting for Accurate but Simplified Models

Traditional 3D modeling was conducted to complement the photogrammetric and Gaussian splatting outputs. Monuments were measured manually using a laser tape and measuring tape, with dimensions plotted on sketches. These sketches were then translated into simplified 3D models (Figure 6 and 7) in SketchUp. While intricate details could not be reproduced with the same fidelity as other methods, the models captured overall volumetric accuracy. Textures were applied manually by observing photographic references.

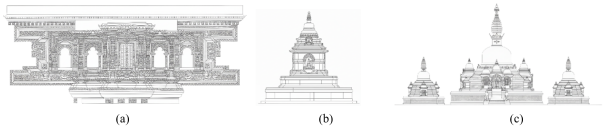

(a) (b) (c)

Figure 6. CAD drafted elevations of (a) Newari Window (b) Chaitya (c) Chilancho Stupa

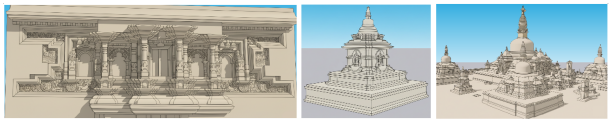

Figure 7. Manual 3d modelling of (a) Newari Window (b) Chaitya (c) Chilancho Stupa

2.4. Data Analysis

2.4.1 Geometric Accuracy

To measure accuracy, the CAD model was taken as the ground truth (control = 0 cm deviation). Reconstructed models from photogrammetry (Reality Scan) and Gaussian splatting (Jawset Postshot) were aligned to the CAD reference using scale markers and transformation tools. Deviations were then recorded at selected control points (corners, edges, and distinctive surface features) in Cloud Compare. The values in the table represent the average deviation in centimeters for each object (Window, Chaitya, Stupa). This provides a direct comparison of how closely each workflow reproduces the CAD reference.

2.4.2 Processing Efficiency

Processing efficiency was evaluated on the same workstation, equipped with AMD Ryzen 7 5800H,16GB RAM, NVIDIA GeForce RTX 3060 Laptop GPU with 6gb VRAM and 2TB NVME SSD, to ensure consistency across workflows. For each model, the total processing time was measured from the start of camera alignment to the final export stage. Memory usage was tracked by monitoring the peak RAM consumption recorded during processing, while GPU load was logged through the NVIDIA system monitor utility. File sizes were recorded from the final exported model outputs. Each workflow was tested in three repeated trials, and the results were averaged to minimize variability. This produced a set of comparable values reflecting the computational intensity of each method.

2.4.3 Cost Analysis

The cost analysis table presents the financial requirements of each workflow in terms of hardware, data acquisition, and processing. Hardware costs represent the one-time purchase of equipment such as cameras, drones, and GPU workstations, but to avoid overstating their impact on individual models these values were amortized over an assumed hardware life of five years and a production rate of 200 models per year. The amortized hardware cost per model was calculated using the Equation 1.

$$\text{Hardware Ammortization} = \frac{\text{Total Hardware Cost}}{\text{Hardware Lifespan} \times \text{Number of models per year}} \quad (1)$$

Data acquisition cost per model includes the recurring fieldwork expenses required to capture each dataset, such as operator labor, travel, and consumables. Processing cost per model accounts for energy consumption and technician time during the computational stage. The total cost per model in the table is then expressed as the sum of these three components, providing a direct measure of the financial burden associated with producing a single model in each workflow.

2.4.4 Usability Assessment

Usability was evaluated through a structured set of tests designed to capture the practical strengths and weaknesses of each workflow. Mesh editability was judged by the time and effort required to perform model cleaning, decimation, and basic edits, with scores ranging from 1 for very limited editability to 5 for fully flexible editing. Virtual Reality (VR) and Augmented Reality (AR) compatibility was tested by exporting the models into Unity and Unreal Engine, where a score of 1 indicated poor compatibility with low frame rates or instability, and 5 indicated seamless real-time integration. Integration with Building Information Modeling (BIM) workflows was assessed by importing models into Revit 2024; scores were based on the amount of rework required, with 1 reflecting significant cleanup and 5 reflecting direct import with minimal adjustment. Scalability was measured by processing larger datasets to observe workflow robustness, where 1 denoted frequent crashes or failures and 5 denoted smooth handling of large-scale scenes. Automation level was assessed by the proportion of the pipeline that could run without user intervention, with 1 representing mostly manual workflows and 5 representing near-complete automation. Finally, visual fidelity was judged by comparing rendered outputs against field photographs, where 1 indicated poor resemblance and lack of detail, while 5 indicated high realism and clarity. Although some criteria involved subjective judgment, the scoring was standardized and applied consistently across repeated trials to ensure reliable comparison between workflows.

3. Results and Discussion

3.1. Geometric Accuracy

Table 1. Comparison of reconstruction accuracy, showing deviations from CAD control (0 cm)

Object	Photogrammetry (cm)	Gaussian Splatting (cm)
Window	$\pm$1.2	$\pm$3.1
Chaitya	$\pm$1.8	$\pm$3.6
Stupa	$\pm$2.3	$\pm$4.5

The results in Table 1 show that photogrammetry yields much lower deviations from the CAD reference than Gaussian splatting: e.g. $\pm$1.2 cm vs $\pm$3.1 cm for the window, and $\pm$2.3 cm vs $\pm$4.5 cm for the stupa. The results suggest that photogrammetry better preserves geometric fidelity, while Gaussian splatting introduces greater error in structural form. This is consistent with comparative studies where Structure-from-Motion/Multi-View Stereo (SfM/MVS) methods outperform view synthesis or rendering-oriented approaches in pure geometric accuracy (Clini et al., 2024). In the comparative analysis of NeRF, Gaussian splatting, and SfM, the authors found that SfM (photogrammetric) reconstructions had the highest geometric precision even though the newer methods achieved faster runtimes (Clini et al., 2024). Thus, our findings align with that trend: photogrammetry remains the more reliable choice when geometric accuracy is critical.

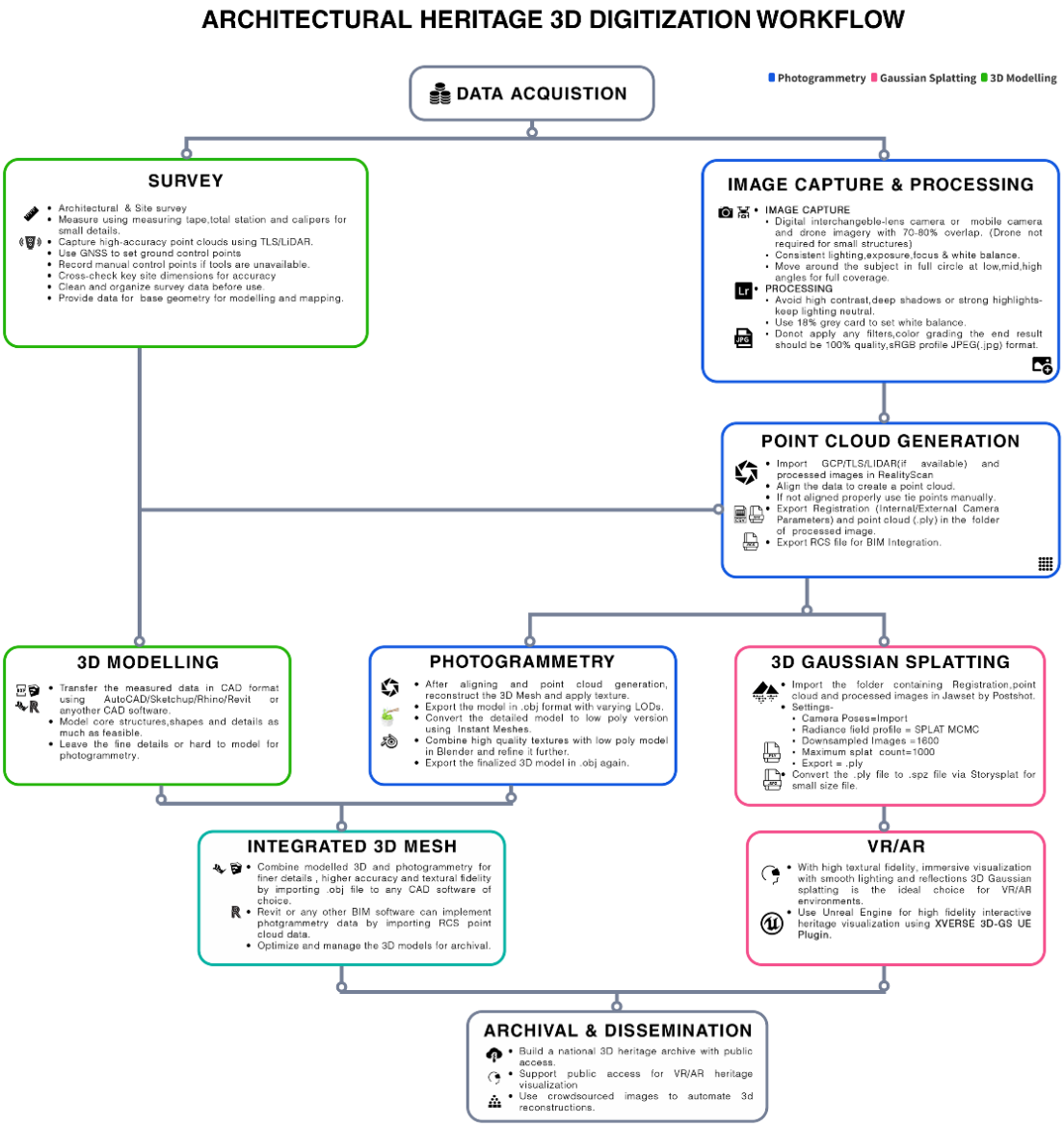

Figure 8. Flowchart for architectural heritage 3D digitization pipeline

3.2. Processing Efficiency

Table 2 reveals that photogrammetry is the most resource-intensive: 180 minutes, 16 GB memory, 96.5 % GPU load, and a large file size (750 MB). Gaussian splatting completes much faster (30 minutes), uses less memory (12 GB), and has moderate GPU load (67.5 %). Manual 3D modeling is extremely slow (1,200 minutes) but imposes lower GPU strain and lower file size (200 MB). The results suggest that Gaussian splatting offers a significant efficiency advantage in real-world scenarios, minimizing computational bottlenecks. This mirrors findings from recent comparative work, where Gaussian splatting converged more quickly and consumed fewer resources than dense SfM/MVS pipelines (Sambugaro et al., 2024). Moreover, photogrammetric workflows are known to saturate GPU and memory during depth-map and densification phases, which matches our high GPU usage

Table 2. Comparison of processing requirements in terms of average time, memory, GPU load and file size

Workflow	Processing Time (min)	Memory Usage (GB)	GPU Load (%)	Mesh File Size (MB)
Photogrammetry	180	16	96.5	750
Gaussian Splatting	30	12	67.5	500
3D Modeling	1200	10	72.5	200

reading (Remondino, 2011). The manual modeling route is inherently labor-driven, so its time cost is dominated by user's skillset and experience rather than hardware.

3.3. Cost Analysis

Cost breakdown in Table 3 demonstrates that, when hardware cost is amortized, photogrammetry's total cost per model is 47,121 NPR, Gaussian splatting 43,131 NPR, and manual 3D modeling 85,245 NPR. The results suggest that Gaussian splatting's efficiency gains offset its hardware burden, yielding the lowest per-model cost. Photogrammetry remains moderately costly but its precision may justify the premium in certain applications. Manual modeling is least efficient per model, largely because its data acquisition and processing (labor) costs remain high and do not scale well. This underscored principle is also observed in the heritage digitization literature: equipment cost becomes negligible per project when amortized over many models, and the dominant factors are recurring time and labor (Peña-Villasenĩn et al., 2024). In contexts where large volumes of models are needed, the cost advantage of Gaussian splatting becomes more pronounced.

3.4. Usability Assessment

In Table 4, the workflows exhibit clear trade-offs. Photogrammetry has moderate mesh editability, good VR/AR compatibility and BIM integration, moderate scalability, medium automation, and solid visual fidelity. Gaussian splatting excels in automation, VR/AR compatibility, and visual fidelity but scores low in mesh editability and BIM integration. Manual 3D modeling leads in editability and BIM integration but lags in automation and visual realism. The results suggest that photogrammetry offers a balanced profile, Gaussian splatting targets high-fidelity visualization and ease of deployment, and manual modeling is ideal when fine control is required. Prior work exploring Gaussian splatting in heritage contexts emphasizes its power in immersive presentation but acknowledges limitations in metric control and post-processing flexibility (Jamil and Brennan, 2025). Therefore, the usability scores reinforce the pattern: use Gaussian splatting for archival visualization, photogrammetry for balanced documentation, and manual modeling for bespoke corrections or complex edits.

4. Architectural Heritage 3D Digitization Workflow

This flowchart depicts a heritage documentation pipeline that begins with data acquisition, subdivided into Survey/TLS and Photography branches. The survey path uses terrestrial scanning or control point measurements to capture structural metrics, while the photography path acquires overlapping high-resolution images under controlled lighting. Next, pre-processing cleans and organizes both datasets. The refined data is fed into Reality Scan for point cloud generation, where TLS and photo datasets are fused or scaled with control references to produce a unified, geometrically accurate point cloud. The workflow then diverges into three complementary streams: 3D modeling (creating structural reconstructions), photogrammetry (dense mesh and texture creation), and Gaussian splatting (radiance-based real-time visualization). Outputs of 3D modeling and photogrammetry merge into an Integrated 3D Mesh, combining precision and detail, while Gaussian splatting yields VR/AR outputs. Finally, both the mesh and visual models are directed into archival & dissemination, envisaging a national heritage repository and public VR/AR access.

5. Conclusion

This study evaluated three workflows photogrammetry (Figure 8), Gaussian splatting, and manual 3D modeling for their effectiveness in the digital documentation of Nepalese architectural heritage. Photogrammetry achieved the highest geometric accuracy, making it suitable for conservation tasks requiring precision, while Gaussian splatting provided exceptional visual fidelity and processing efficiency for archival and immersive applications. Manual 3D modeling, although labor-intensive, offered strong editability and BIM integration. Collectively, these findings demonstrate that each method contributes distinct advantages that, when integrated, form a balanced and efficient approach to heritage digitization.

Accordingly, this study proposes a hybrid workflow that integrates these complementary methods into a unified digital heritage pipeline. The proposed system envisions a national 3D digitization platform capable of hosting photogrammetric models and Gaussian splat renderings within an accessible repository. Through crowdsourced image contributions and VR/AR visualization, this workflow would not only enhance accuracy and scalability but also promote long-term preservation, public engagement, and sustainable digital heritage

Table 3. Comparison of cost per model output based on amortized hardware, data acquisition and processing/modelling costs.

Workflow	Hardware Cost (NPR)	Hardware Amort./model (NPR)	Data Acquisition/model (NPR)	Processing/model (NPR)	Total Cost/model (NPR)
Photogrammetry	471,000	471	40,000	6,650	47,121
Gaussian Splatting	471,000	471	40,000	2,660	43,131
3D Modeling (manual)	245,000	245	60,000	25,000	85,245

Table 4. Qualitative assessment of workflows across different factors, scored from 1 (low) to 5 (high)

Workflow	Mesh Editability (1–5)	VR/AR Compatibility (1–5)	BIM Integration (1–5)	Scalability (1–5)	Automation Level (1–5)	Visual Fidelity (1–5)
Photogrammetry	3	4	4	3	3	4
Gaussian Splatting	2	5	2	4	5	5
Integrated Mesh	5	5	5	4	2	3

management in Nepal.

References

Angelini, P., et al. (2016). Title not provided in source. *Not specified*.

Champion, E. (2015). *Critical gaming: Interactive history and virtual heritage*. Routledge. https://doi.org/10.4324/9781315587963

Clini, P., Nespeca, R., Angeloni, R., & Coppetta, L. (2024). 3d representation of architectural heritage: A comparative analysis of nerf, gaussian splatting, and sfm-mvs reconstructions using low-cost sensors. *ISPRS Archives of Photogrammetry, Remote Sensing and Spatial Information Sciences*, *XLVIII-2/W8*, 93–99. https://doi.org/10.5194/isprs-archives-XLVIII-2-W8-2024-93-2024

Gudon, A., & Lepetit, V. (2024). Sugar: Surface-aligned gaussian splatting for efficient 3d mesh reconstruction and high-quality mesh rendering. *Proceedings of the IEEE/CVF Conference on Computer Vision and Pattern Recognition (CVPR)*, 10345–10355.

Jamil, O., & Brennan, A. (2025). Immersive heritage through gaussian splatting: A new visual aesthetic for reality capture. *Frontiers in Computer Science*, *7*, 1515609. https://doi.org/10.3389/fcomp.2025.1515609

Letellier, R. (2007). *Recording, documentation, and information management for the conservation of heritage places: Guiding principles*. Getty Conservation Institute. https://www.getty.edu/publications/heritagerecording

Peña-Villasenĩn, S., Gil-Docampo, M., Ortiz-Sanz, J., Vilas Boas, L., Bettencourt, A. M. S., & Cabanas, M. F. (2024). Sfm photogrammetry for cost-effective 3d documentation and rock art analysis of the dombate dolmen (spain) and the megalithic sites of chãos dos cabanos and chãos da escuselha (portugal). *Remote Sensing*, *16*(18), 3480. https://doi.org/10.3390/rs16183480

Remondino, F. (2011). Heritage recording and 3d modeling with photogrammetry and 3d scanning. *Remote Sensing*, *3*, 1104–1138. https://doi.org/10.3390/rs3061104

Sambugaro, Z., Orlandi, L., & Conci, N. (2024). 3d reconstruction methods in industrial settings: A comparative study for colmap, nerf, and 3d gaussian splatting. *CEUR Workshop Proceedings*, *3762*, 242–247. http://ceur-ws.org/Vol-3762/531.pdf

Tiwari, S. R. (2009). *Temples of the nepal valley*. Himal Books.

Westoby, M. J., Brasington, J., Glasser, N. F., Hambrey, M. J., & Reynolds, J. M. (2012). Structure-from-motion photogrammetry: A low-cost, effective tool for geoscience applications. *Geomorphology*, *179*, 300–314. https://doi.org/10.1016/j.geomorph.2012.08.02

This work is licensed under a Creative Commons "Attribution-NonCommercial-NoDerivatives 4.0 International" license.

Published by JScE as Proceedings of 4th International Conference on Earthquake Engineering and Post-Disaster Reconstruction Planning (ICEE-PDRP), 19-21 Jan. 2026, Bhaktapur, Nepal

This page is intentionally left blank.